Supporting Information on "A Field Evidence Model: How to Predict Transport in a Heterogeneous Aquifers at Low Investigation Level?"

Alraune Zech, Peter Dietrich, Sabine Attinger, Georg Teutsch

January 21, 2020

Overview on Field Data at MADE site

Table 1: Summary of observation data on hydraulic conductivity at MADE site with number of campaigns in brackets.

Method of Measurement	**References**
Groundwater level monitoring (1)	*Boggs et al.* [1990]
Soil Sampling (2)	*Boggs et al.* [1990]; *Rehfeldt et al.* [1992]; *Bianchi et al.* [2011b]
Pumping Tests (1)	*Boggs et al.* [1990]
Slug tests (1)	*Boggs et al.* [1990]
Packer Tests (1)	*Boggs et al.* [1990]
Permeameter Tests (1)	*Boggs et al.* [1990]
Borehole Flowmeter (3)	*Rehfeldt et al.* [1989]; *Boggs et al.* [1990, 1993, 1995]
DPIL, DPP (2)	*Liu et al.* [2009]; *Bohling et al.* [2012]
Surface Geophysics (2)	*Boggs et al.* [1990]; *Bowling et al.* [2005]
Natural Gradient Tracer Test (MADE-1, MADE-2, MADE-3)	*Boggs et al.* [1992]; *Rehfeldt et al.* [1992]; *Boggs et al.* [1993, 1995]; *Julian et al.* [2001]
Force Gradient Tracer Test (MADE-4, MADE-5)	*Liu et al.* [2010]; *Bianchi et al.* [2011a]

Details on Hydraulic Conductivity Structure A

Module (A) for MADE comprises of two deterministic zones whose presence is indicated by the piezometric surface map (Figure 1a) and two large scale pumping tests (Figure 3a) [*Boggs et al.*, 1992]. Zone Z_1 is an area of low conductivity from upstream of the tracer input location to $x = 20\,\mathrm{m}$ downstream with a specific mean value of $\bar{K}_{Z1} = 2e-6\,\mathrm{m/s}$. Zone Z_2 is a high-in-the-average conductivity area upstream beyond 20 m from the source location with a mean conductivity of $\bar{K}_{Z2} = 2e - 4\,\mathrm{m/s}$.

The value of $\bar{K}_{Z2}$ is the outcome of a large scale pumping test [*Boggs et al.*, 1990]. The test was performed about 60 m downstream of the source location within the distribution area of the tracer plume (Figure 3a). Conductivity estimates for different observation wells reveal little spread. Thus, the test's support area is of relatively uniform high conductivity.

The conductivity in zone Z_1 is critical because the value in the vicinity of the tracer injection area determines the early plume development. *Boggs et al.* [1990] reported a mean conductivity of $2e - 5\,\mathrm{m/s}$ for a large scale pumping test AT1 which was performed about 90 m upstream of the source location (Figure 3a), thus outside of the tracer distribution area. The conductivity values from the individual observations wells show a large spread indicating strong heterogeneity within this area. Furthermore, pumping tests tend to emphasize the impact of high conductivity areas, possibly overestimating the mean conductivity.

Since the tracer injection site is not located within the support volume of the pumping tests AT1, we consider additional data taken during tracer injection. Water levels were monitored manually in the injection wells and seven observation wells close to the source [*Boggs et al.*, 1990]. A pressure head increase of more then 0.5 m up to 0.64 m was observed in all injection wells. Combining the head increase with the mean injection rate of $Q_{in} = 1.15e-5\ \mathrm{m^3/s}$ indicates a conductivity of $\bar{K}_{Z1} = 2e - 6\,\mathrm{m/s}$ in the source area.

Details on Flow and Transport Model Settings

The simulation domain is a 2D cross section within $x \in [-20, 200]\,\mathrm{m}$ and $z \in [52, 62]\,\mathrm{m}$ generously comprising the area of the MADE-1 tracer experiment [*Boggs et al.*, 1992]. The grid has a resolution of $\Delta x = 0.25\,\mathrm{m}$ and $\Delta z = 0.05\,\mathrm{m}$. The temporal resolution is one day. Flow boundary conditions are no flow at top and bottom of the domain and a constant head of $h = 63\,\mathrm{m}$ at the left and $h = 62.34\,\mathrm{m}$ at the right, resulting in mean had gradient of $J = 0.003$. The porosity was set to 0.32.

The tracer input takes place at a central injection well located at $x = 0$ with a screen of 0.6 m length at $z \in [57.2, 57.8]\,\mathrm{m}$. Tracer was injected over 48.5 h with forced input conditions of an injection rate of $Q_{in} = 1.166e - 5\,\mathrm{m^3/s}$.

Details on Parametric Uncertainty for Binary Structure A+B

Figure 1 shows the longitudinal mass distributions for different combination of input parameters for the binary inclusion structure (A+B). Within every panel, one parameter was varied in comparison to the standard parameter choice of $K_{Z1} = 2e - 6\,\mathrm{m/s}$; $K_{Z2} = 2e - 4\,\mathrm{m/s}$; $p = 15\%$; $I_l = 10\,\mathrm{m}$; $I_v = 0.5\,\mathrm{m}$ $x_I = 20\,\mathrm{m}$.

The inclusion length and the choice of the K contrast between the zones show the highest impact. The later was to be expected as the mean conductivity determines the average flow velocity and thus the peak location and the general distribution shape.

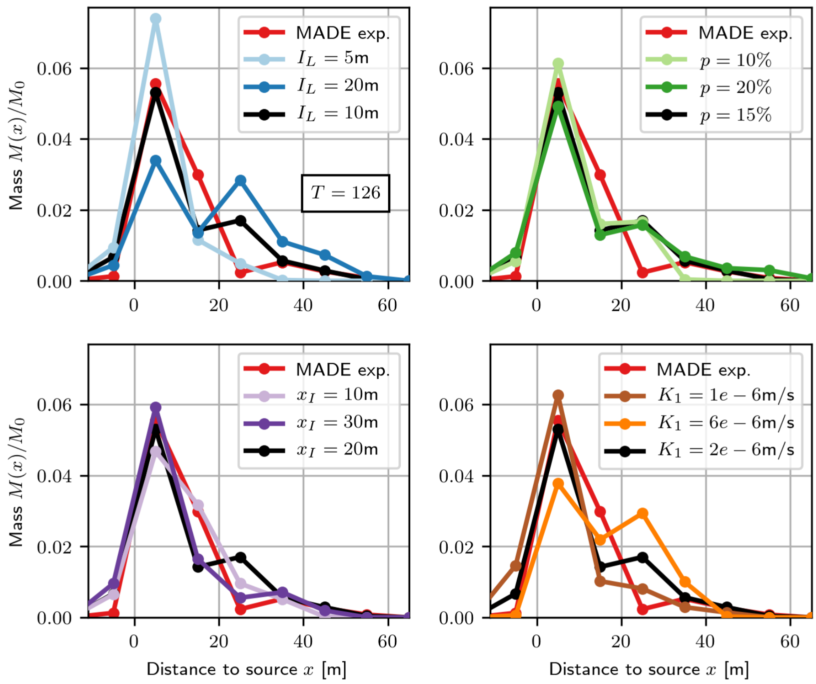

Figure 1: Mass distribution at $T = 126$ days for conductivity concept (A+B), inclusions in zones for various input parameter combinations: for inclusion length I_L , amount of inclusions p, distance of zone interface x_I to source location and mean conductivity K_1 of zone Z_1 (source area). MADE experiment observations in red.

The horizontal inclusion length I_h determines the connectivity of the source area to the high conducitivity zone. Thus, the larger I_h the higher is the amount of mass transported downstream, visible a the lower mass peak value at $x = 5$,m and higher second peak at $x = 25$,m for $I_h = 20$ m in Figure 1a. The uncertainty bands in Figures 6b and 7 (main paper) coincide with the upper and lower range given by the ensemble results for $I_h = 5$ m and $I_h = 20$ m.

Other parameters as the distance of the interface to the injection location x_I (Figure 1c), the amount of inclusion p (Figure 1b) as well as the vertical inclusion length I_v have minor effects. Similarly, the choice of sub-scale heterogeneity parameters is secondary since the inclusion structure dominates the mass distribution. We tested values up to $\sigma^2 = 2$ and found nearly no difference to the results of the standard setting for the conductivity concept (A+B+C).

In general, all parameter combinations within the value ranges determined for MADE (section **??**) show a similar mass distribution pattern. In this regard, the binary structure is very stable towards parametric uncertainty.

References

Bianchi, M., C. Zheng, G. R. Tick, and S. M. Gorelick, Investigation of Small-Scale Preferential Flow with a Forced-Gradient Tracer Test, *Ground Water*, *49*(4), 503–514, doi:10.1111/j.1745-6584.2010.00746.x, 2011a.

Bianchi, M., C. Zheng, C. Wilson, G. R. Tick, G. Liu, and S. M. Gorelick, Spatial connectivity in a highly heterogeneous aquifer: From cores to preferential flow paths, *Water Resour. Res.*, *47*(5), W05,524, doi:10.1029/2009WR008966, 2011b.

Boggs, J. M., S. Young, D. Benton, and Y. Chung, Hydrogeologic Characterization of the MADE Site, *Tech. Rep. EN-6915*, EPRI, Palo Alto, CA, 1990.

Boggs, J. M., S. C. Young, L. M. Beard, L. W. Gelhar, K. R. Rehfeldt, and E. E. Adams, Field study of dispersion in a heterogeneous aquifer: 1. Overview and site description, *Water Resour. Res.*, *28*(12), 3281–3291, doi:10.1029/92WR01756, 1992.

Boggs, J. M., L. M. Beard, W. Waldrop, T. B. Stauffer, W. G. MacIntyre, and C. P. Antworth, Transport of Tritium and Four Organic Compounds During a Natural-Gradient Experiment (MADE-2), *Tech. Rep. TR-101998*, EPRI, Palo Alto, CA, 1993.

Boggs, J. M., J. Schroeder, and S. Young, Data to support model development for natural attenuation study, *Tech. Rep. WR28-2-520-197*, TVA Engineering Laboratory, Tennessee Valley Authority, Norris, Tennessee, 1995.

Bohling, G. C., G. Liu, S. J. Knobbe, E. C. Reboulet, D. W. Hyndman, P. Dietrich, and J. J. Butler, Geostatistical analysis of centimeter-scale hydraulic conductivity variations at the MADE site, *Water Resour. Res.*, *48*, W02,525, doi:10.1029/2011WR010791, 2012.

Bowling, J. C., A. B. Rodriguez, D. L. Harry, and C. Zheng, Delineating alluvial aquifer heterogeneity using resistivity and GPR data, *Ground Water*, *43*(6), 890–903, doi:10.1111/j.1745-6584.2005.00103.x, 2005.

Julian, H. E., J. M. Boggs, C. Zheng, and C. E. Feehley, Numerical simulation of a natural gradient tracer experiment for the natural attenuation study: Flow and physical transport, *Ground Water*, *39*(4), 534–545, doi:10.1111/j.1745-6584.2001.tb02342.x, 2001.

Liu, G., J. J. Butler, G. C. Bohling, E. Reboulet, S. Knobbe, and D. W. Hyndman, A new method for high-resolution characterization of hydraulic conductivity, *Water Resour. Res.*, *45*(8), W08,202, doi:10.1029/2009WR008319, 2009.

Liu, G., C. Zheng, G. R. Tick, J. J. Butler, and S. M. Gorelick, Relative importance of dispersion and rate-limited mass transfer in highly heterogeneous porous media: Analysis of a new tracer test at the Macrodispersion Experiment (MADE) site, *Water Resour. Res.*, *46*(3), W03,524, doi:10.1029/2009WR008430, 2010.

Rehfeldt, K. R., P. Hufschmied, L. W. Gelhar, and M. Schaefer, Measuring hydraulic conductivity with the borehole flowmeter, *Tech. Rep. EN-6511*, EPRI, Palo Alto, CA, 1989.

Rehfeldt, K. R., J. M. Boggs, and L. W. Gelhar, Field study of dispersion in a heterogeneous aquifer: 3. Geostatistical analysis of hydraulic conductivity, *Water Resour. Res.*, *28*(12), 3309–3324, doi:10.1029/92WR01758, 1992.